scientific reports

Check for updates

OPEN

A molecular network analysis and in silico docking of beta-eudesmol, atractylodin and hinesol in patients with advance stage intrahepatic cholangiocarcinoma

Teerachat Saeheng[1,2], Ethan Vindvamara[2], Wanna Chaijaorenkul[1,2], Nisit Tongsiri[3] & Kesara Na-Bangchang[1,2,3]✉

Cholangiocarcinoma (CCA), the bile duct cancer, is associated with a high burden and poor prognosis. This is due to the lack of early diagnostic tools and effective chemotherapy. Molecular networking is a promising tool for investigating the molecular mechanisms of drugs or candidate molecules for various diseases. This study investigated molecular targets and signaling pathways of the three components (atractylodin, beta-eudesmol, and hinesol) of *Atractylodes lancea* Thunb. (DC.) (AL), the promising candidate for patients with advanced-stage intrahepatic CCA (iCCA). The independent-sample T-test or Mann-Whitney U test was used to identify significant gene targets in (i) patients with advanced-stage iCCA who received AL treatment and those who received palliative care alone, and (ii) patients with progressive and non-progressive diseases. A molecular network was constructed using Cytoscape to identify AL signaling action pathways. Fifty-two genes were identified as the essential targeted genes in patients with advanced-stage iCCA. The most critical gene hubs were TNFα (1st rank), NRAS (2nd rank), and PI3KCA (3rd rank). The false discovery rate (FDR) identified PI3K/AKT, NK cell-mediated cytotoxicity, and apoptosis as the top three significant pathways. Hinesol showed the highest binding affinity compared with other components of AL and the standard anti-CCA drugs gemcitabine and 5-FU. Molecular networking is a valuable tool for investigating molecular signaling networks of herbal medicine with multiple active and non-active ingredients. With multi-signaling targets linked to all tumor development and progression stages, the study supports AL as a promising candidate for patients with advanced-stage iCCA.

Keywords Molecular network, *Atractylodes lancea* Thunb (DC.), Traditional medicine, Cholangiocarcinoma

Cholangiocarcinoma (CCA) is an aggressive malignancy often diagnosed in elderly patients who may not tolerate traditional chemotherapy due to adverse reactions and comorbidities. This highlights the need for alternative treatments. Atractylodes lancea (Thunb.) DC (AL), a traditional herb used in East Asia, shows promise as a novel CCA therapy. Active components like atractylodin and beta-eudesmol exhibit antiproliferative, anti-angiogenic, and anti-metastatic effects in preclinical studies[1,2]. Recent research highlights synergistic interactions between AL's bioactive constituents, such as beta-eudesmol, atractylodin, and hinesol, with favorable fractional inhibitory concentration (FIC) values[3]. These compounds induce G1 cell cycle arrest and apoptosis in CCA cells by modulating p21 expression[4]. Beta-eudesmol also sensitizes chemotherapy-resistant CCA cells to agents like 5-FU and doxorubicin by altering the Bax/Bcl-2 ratio and suppressing NQO1 expression[5]. It inhibits CCA cell migration by suppressing the epithelial-mesenchymal transition (EMT) pathway and downregulates the PI3K-AKT signaling pathway[6]. In zebrafish models, beta-eudesmol shows anti-angiogenic effects by inhibiting Vegfa

[1]Centre of Excellence in Pharmacology and Molecular Biology of Malaria and Cholangiocarcinoma, Chulabhorn International College of Medicine, Thammasat University (Rangsit Campus), 99 moo 18, Phaholyothin Road, Klong Luang District, Pathumthani 12121, Thailand. [2]Gradulate Program in Bioclinical Science, Chulabhorn International College of Medicine, Thammasat University (Rangsit Campus), Klong Luang District, Pathumtanee province, Thailand. [3]Sakol Nakorn Hospital, Sakol Nakorn, Sakol Nakorn Province, Thailand. ✉email: kesaratmu@yahoo.com; nkesara@tu.ac.th

and Vegfr2[7]. In vivo studies in a CCA hamster model further support these findings, showing modulation of apoptosis-related genes[8].

Molecular networking, used in exploring drug and herbal interactions, has been applied in various diseases like rheumatoid arthritis[9], hepatocellular carcinoma[10], and colorectal cancer[11]. While clinical trials have confirmed AL's efficacy and safety in CCA treatment[6], the detailed molecular mechanisms remain unclear.

This study aims to apply molecular networking to identify gene targets and signaling pathways modulated by AL in advanced-stage intrahepatic CCA (iCCA). It will focus on: (i) constructing a gene ontology based on statistical analysis, (ii) identifying key gene targets through molecular network and functional enrichment analysis, and (iii) evaluating the binding affinity of AL's active compounds using in silico docking simulations. This approach will enhance understanding of AL's mechanisms and its potential as a CCA therapeutic agent.

Methods

Study design, patients, and study procedures

This study is part of a phase IIA open-label, randomized controlled trial assessing the dose, pharmacokinetics, safety, and efficacy of *Atractylodes lancea*(AL) in patients with advanced-stage intrahepatic cholangiocarcinoma (iCCA)[12] [01/03/2021; TCTR20210129007; ICTRP Search Portal (who.int)]. The protocol was approved by the Ethics Committee of Sakol Nakorn Hospital (No. 049/2021) and conducted in compliance with the Helsinki Declaration. Informed consent was obtained from all participants. The AL treatment regimen included: Group 1 ($n=6$): 1,000 mg daily of standardized AL extract for 90 days with standard care; 5 with non-progressive disease, 1 with progressive disease; Group 2 ($n=5$): Dose escalation from 1,000 mg to 2,000 mg over 90 days with standard care; 3 with non-progressive disease, 2 with progressive disease; and Group 3 ($n=4$): Standard care alone; 3 with progressive disease, 1 with non-progressive disease.

Blood samples (3 mL) were collected on days 1 and 28. Plasma was isolated and stored at −80 °C for analysis. RNA was extracted from whole blood, and gene expression was analyzed using the nCounter PanCancer Pathways Panel (NanoString Technologies, Seattle, US), which covered 730 genes linked to 13 cancer-related pathways. The ratios of gene expression between day 28 and day 1 were analyzed to identify significant signaling pathways and differences between progressive and non-progressive disease, as well as survivors and non-survivors.

Analysis of the association between gene expression and AL treatment

Gene expression analysis in response to AL treatment involved a comprehensive network analysis using functional enrichment through Gene Ontology (GO), Kyoto Encyclopedia of Genes and Genomes (KEGG) pathways, and Reactome. The comparisons included: (i) AL treatment (Groups 1 and 2) vs. non-treatment (Group 3), (ii) disease progression (progressive vs. non-progressive disease after AL treatment), and (iii) survival (survived vs. non-survived patients post-treatment). Data normality was assessed using the Shapiro-Wilk test, with the independent-sample T-test for normally distributed variables and the Mann-Whitney U test for non-normally distributed variables. The exact p-values were reported using SPSS version 23.

Genes with significant expression changes were selected for molecular network analysis. The biological process was the primary focus of molecular network analysis, as it captures the coordinated actions of molecular functions that collectively achieve biological objectives. This approach provides a deeper understanding of the molecular mechanisms at play compared to examining individual molecular functions in isolation.

Protein-protein interaction (PPI) networks were constructed using Cytoscape, following these steps: (i) identification of significant gene expression variations between the AL-treated and control groups; (ii) access to the STRING database, selecting Homo sapiens and full STRING networks with a confidence score cut-off of 0.4; (iii) importing gene expression data, including gene types, ratios, and p-values; (iv) functional enrichment analysis through the cytoNCA plugin, which calculates betweenness, closeness, and degree centralities; and (v) iltering results to select KEGG pathways, Reactome pathways, and GO biological processes.

In the network, "degree" indicates a node's direct connections, highlighting its role as a central hub. "Betweenness centrality" measures how often a node lies on the shortest path between pairs of nodes, while "closeness centrality" indicates how efficiently a node connects to others in the network.

GO and pathway enrichment analyses were performed using Cytoscape 3.1.0 to visualize and annotate the results. Fisher's exact test was used to select pathways involving at least three candidate genes, with statistical significance set at $p<0.05$ and a false discovery rate (FDR) cut-off of $p<0.05$. The PPI network and pathway enrichment analysis leveraged STRING confidence scores and FDR values to identify significant protein interactions and associated pathways.

The associations between biomarkers and the fold changes of gene expressions in patients with disease progression (progressive and non-progressive diseases) or survival status (survivors and non-survivors)

Independent t-test (for normally distributed data) and Mann Whitney U test (for non-normally distributed data) were used to compare the differences in biomarkers (fold changes in biomarker levels and mRNA expression) between the groups of patients with progressive and non-progressive diseases, as well as between those who survived and did not survive.

Pearson correlation test (for normally distributed data) and Spearman's correlation test (for non-normally distributed data) were used to determine the correlation between biomarkers (fold changes in biomarker levels and mRNA expression) in the groups of patients with progressive and non-progressive diseases, as well as in those who survived and did not survive.

The statistical significance level was set at $\alpha=0.05$ for all tests.

ROC analysis, cut-off value, and model performance

Receive Operating Curve (ROC) was applied to determine the cut-off levels for significant levels of mRNA expressions between the groups of patients with progressive and non-progressive disease and those who survived and did not survive. Area Under Curve (AUC) of ≥ 0.7 was the predefined criterion for identifying substantial mRNA expressions between progressive and non-progressive diseases and survivors and non-survivors. A p-value of ≤ 0.05 was set as a statistically significant level. The Youden's index was employed to determine the optimal cut-off value. Sensitivity, specificity, accuracy index, Negative predictive value (NPV), and positive predictive value (PPV) were computed to indicate the model's performance.

Kaplan-Meier analysis

The designated cut-off value for each important gene was used to categorize the significant genes into two groups, i.e., ratios above or below the threshold. The Kaplan Meier assessed the impact of mRNA expression (disease progression and survival status) above or below the threshold on progression-free survival time (PFS) and overall survival (OS). A log-rank test was applied to determine the significant differences between ratios (above or below threshold) on PFS and OS with the predefined p-value of ≤ 0.05.Pathway cross-talk analysis.

The Jaccard index was used to assess the reliability of cross-talk analysis. The inclusion criterion was a pathway with ≥2 candidate genes (to exclude genes with inadequate biological information) and the exclusion criterion was the pair of pathways with < 2 shared candidate genes. The selected pair of pathways were prioritized based on the Jaccard index of > 0.25 and > 0.6 for pathway-pathway interaction and pathway redundancy, respectively[13].

In silico docking simulation of gene targets

In silico docking simulations were conducted using AutoDock software to evaluate the binding affinities of Atractylodes lancea (AL) compounds (atractylodin, beta-eudesmol, and hinesol), standard anti-CCA drugs (5-FU and gemcitabine), and reference compounds to ten significant target proteins: JAK1, PI3KCA, HDAC2, ILR2A, ILR2B, TNF-α, SMAD2, NRAS, SOS1, ERRB2, and DMT3A. The crystallographic structures of the AL target proteins were retrieved from the RCSB Protein Data Bank, and the active compound structures were obtained from the PubChem database in SDF format, then converted to PDB files using PyMOL or OpenBabel.

A free energy force field was calculated using a Lamarckian Genetic Algorithm to predict the binding affinity based on the Gibbs free energy. Docking was performed with the catalytic domain of each receptor to interact with the small ligands (Table S1). The optimal docking conformation was selected based on the ligand conformation with the lowest root-mean-square deviation (RMSD) using a tolerance of 2.0 Å. A binding affinity of ≥ 6 kcal/mol was considered acceptable. 5-FU and gemcitabine were chosen for docking simulations as they are first-line treatments for intrahepatic cholangiocarcinoma (iCCA).

Results

Baseline characteristics

The diagrammatic workflow in this study is shown in Fig. 1. Table 1 summarizes the baseline characteristics of the patients with advanced-stage iCCA in each treatment group (group 1 and group 2) and the control group (group 3). No significant differences between AL-treated patients with progressive and non-progressive diseases were observed with age ($p = 0.843$), body weight ($p = 0.278$), height ($p = 0.768$), white blood cell count ($p = 0.212$), platelet count ($p = 0.125$), hemoglobin ($p = 0.105$), INR ($p = 0.914$), PT ($p = 0.753$), PTT ($p = 0.694$), creatinine clearance ($p = 0.471$), AST ($p = 0.053$), ALT ($p = 0.078$), ALP ($p = 0.809$), CPK ($p = 0.103$), LDH ($p = 1.00$), CA19-9 ($p = 0.661$), CEA ($p = 0.177$), and IL-6 ($p = 0.343$) between the treatment and control groups. Subgroup analysis revealed no significant changes in baseline AST ($p = 0.842$), ALT ($p = 0.630$), ALP ($p = 0.352$), LDH ($p = 0.376$), CPK ($p = 0.09$), CA19-9 ($p = 0.497$), CEA ($p = 1$), and IL6 ($p = 0.683$) levels. The comparable values between survivors and non-survivors in the AL-treated group were not substantially different [(AST, $p = 0.145$), (ALT, $p = 0.352$), (ALP, $p = 0.886$), (LDH, $p = 1.00$), (CPK, $p = 0.327$), (CA19-9, $p = 1.00$), (CEA, $p = 0.727$), and (IL6, $p = 0.183$).

Association between gene expression and AL treatment

Out of 730 genes analyzed, 52 showed significant changes in gene expression levels following AL treatment (Fig. 2). PRKAR2A, SPOP, RXRG, FGF1, PAX8, TNFRSF10A, and TCFL1 genes showed high gene expression levels, while the remaining showed relatively low expression levels. Further analysis revealed a marked difference in the expression levels of 16 gene targets in patients with progressive and non-progressive disease following AL therapy (Group 1 and 2). BDNF, ERBB2, TTK, and XPA showed higher expression levels, while the remaining showed lower expression levels. Seven genes were identified with marked differences between survivors and non-survivors. HSPA1A, FOS, CBL, and MMP9 were the top four upregulated genes. Tables S2, S3 and S4 summarize significant gene expressions (fold-change) between AL-treated and control group, and patients with progressive and non-progressive diseases, and survivors and non-survivors, respectively.

Proposed molecular signaling pathways of AL action in advanced-stage iCCA

A comprehensive network analysis in AL-treated (Groups 1 and 2) and control (Group 3) identified 44 potential target genes. Thirty genes were identified as core hubs (Table 2). TNF-α was the network's most significant hub (PPI = 22), followed by PIK3CA (PPI = 15), NRAS (PPI = 14), JAK1 (PPI = 11), IL2RB (PPI = 11), and IL2RA (PPI = 11). Subsequent network interaction analysis revealed 44 nodes and 115 edges (PPI = 5.18).

Based on pathway enrichment analysis, AL action (specific condition or disease) was significantly linked with various signaling pathways, i.e., PI3K-AKT, NK cell-mediated cytotoxicity, cellular apoptosis, MAPK, JAK-STAT and NF-kB in cancer, EGFR-resistance, focal adhesion, Fc epsilon RI, T cell receptor, cell senescence, regulation of actin cytoskeleton, transcription misregulation, B cell receptor, mTOR, ERBB, Ras, VEGFR, PDL-1, RIG-I-

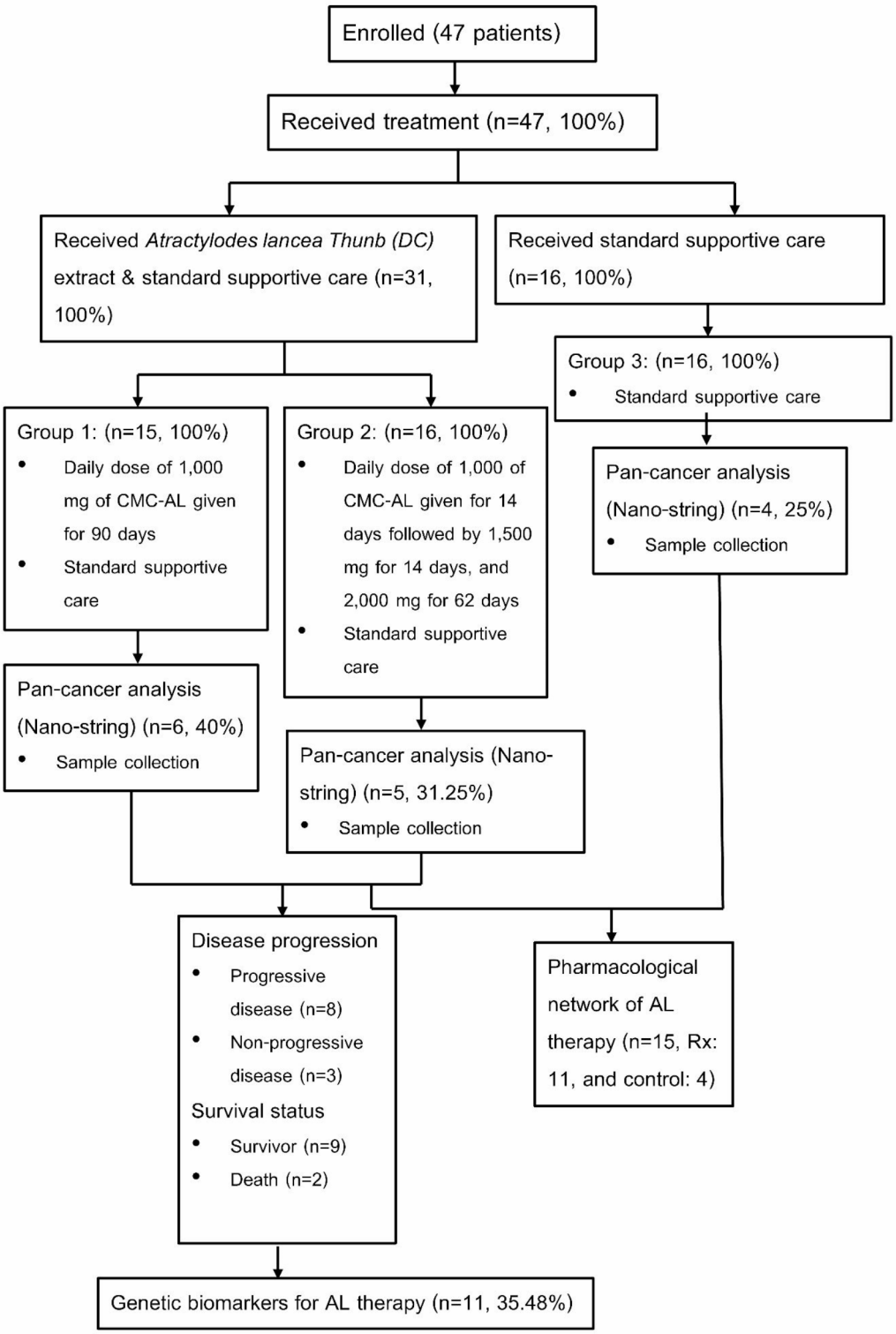

Fig. 1. The diagramtic flow chart of the study.

like receptor, platinum drug resistance, and P53 signaling pathways (Fig. 3). Comprehensive network analysis using Reactome database identified 38 multiple signaling pathways, i.e., signal transduction, IL2, IL3, IL4, IL5, IL13, GM-CSF, ILR SHC, extra-nuclear estrogen, FGFR3 in disease, downstream signaling of activated FGFR1-4, DAP12, death receptor, FLT3, PDGFRA, and EGFR-v-III. These pathways were linked with 180 biochemical pathways. Functional enrichment analysis of the 20 selected biological processes based on the set criterion, i.e., KEGG, biological processes, and Reactome are shown in Figs. 3 and 4, and 5, respectively. The set criterion

Demographic data	Treatment ($n=11$)	Control ($n=4$)
Sex	M: 7 (63.64%) F: 4 (36.36%)	M: 1 (25%) F: 3 (75%)
Age (year)	67.58 (95%CI: 61.99–73.17)	65 (95%CI: 59.42–77.55)
Body weight (Kg)	54.03 (95%CI: 48.121–59.94)	50.1 (95%CI: 23.47–76.72)
Height (cm.)	157.6 (95%CI: 152.72–157.44)	156 (95%CI: 134.53–177.67)
Staging		
• IIIB	0 (0%)	1 (25%)
• IV	11 (100%)	3 (75%)
ECOG score		
• 0–1	6 (54.54%)	1 (25%)
• 2	5 (45.46%)	3 (75%)
WBC (x10^3 cells/μL)	9.23 (95%CI: 6.64–12.02)	7.49 (95%CI: 2.65–12.34)
Platelets (x10^3 cells/μL)	308.58 (95%CI: 239.34–377.82)	203.5 (95%CI: 2.944–409.94)
Hb (g/dL)	11.80 (95%CI: 10.84–12.76)	10.42 (95%CI: 7.03–13.82)
PT (seconds)	13.22 (3.4)	13.55 (95%CI: 10.41–16.69)
INR	1.14 (95%CI: 1.02–1.26)	1.13 (95%CI: 0.92–1.34)
PTT (seconds)	28.61 (95%CI: 25.68–31.52)	29.52 (95%CI: 26.52–32.53)
Creatinine clearance (mL/min)	52.16 (95%CI: 42.54–61.78)	60.25 (95%CI: 14.60–105.89)
AST (IU/L)	118.67 (95%CI: 59.39–177.94)	49.75 (95%CI: 28.24–71.25)
ALT (IU/L)	45 (100)	17 (17.25)
ALP (IU/L)	295.8 (95%CI: 199.57–458.63)	270.75 (95%CI: 60.33–601.83)
LDH (IU/L)	527 (313.2)	622. 62 (95%CI: 148.22–1097.03)
CPK (μg/L)	97.27 (95%CI: 67.68–147.33)	48.63 (95%CI: 11.98–109.23)
CA19-9 (U/L)	322 (2336)	2042 (95%CI: 2914–7000.08)
CEA (pg/L)	4.8 (14.35)	411.67 (95%CI: 414–1237)
IL6 (pg/mL)	36.11 (95%CI: 22.46–49.75)	13.45 (20.33)

Table 1. Demographic data, baseline hematological and biochemical characteristics. Data are presented as N (%) or mean (95%CI) or median (IQR).

included the three shared genes with a p-value of ≤ 0.05 between signaling pathways for representing the KEGG, biological, and Reactome processes. A pharmacological mechanism of AL is shown in Fig. 6.

The associations between biomarkers and the fold changes of mRNA expressions in patients with disease progression and survival status, Kaplan-Meier analysis, and cox-proportional regression analysis

Disease progression

The study assessed the relationship between proposed biomarkers and mRNA expression changes in patients experiencing disease progression and survival status through Kaplan-Meier and Cox-proportional regression analyses.

A significant difference in ALP ratios was observed between patients with progressive and non-progressive disease, with a p-value of 0.048. Other biomarkers (AST, ALT, LDH, CPK, CA19-9, CEA, and IL-6) did not show significant associations (Table S5). The ROC analysis indicated that the cut-off value for ALP ratios to distinguish between disease progression was ≥ 1.023 folds (AUC = 0.917, 95% CI = 0.739–1.00, $p = 0.04$; Youden's index = 0.875) (Fig S1). This yielded a sensitivity of 87.5%, specificity of 100%, positive predictive value (PPV) of 1, negative predictive value (NPV) of 0.75, and accuracy index (AI) of 0.9. However, Kaplan-Meier analysis revealed significant no differences in progression-free survival (PFS) based on these ALP ratios ($p = 0.104$) (Fig S2). No significant difference following cox-proportional regression analysis was found disease progression and ALP ratios (HR: 5.27, 95%CI: 0.89–100.6, $p = 0.1265$) (high vs. low) (Fig S3).

The ROC analysis for various genes indicated significant differences in their expression between progressive and non-progressive disease: APC (≥ 1.49 folds, AUC = 0.917, $p < 0.001$), BAX (≥ 0.82 folds, AUC = 0.917, $p < 0.001$), DNMT3A (≥ 0.805 folds, AUC = 1, $p < 0.001$). Others included ETS2, GNA11, IGF1, IRAK2, PLCG2, POLB, RAF1, THEM4, BDNF, CDKN2A, ERBB2, TTK, and XPA, with respective AUC values indicating strong predictive capability (AUCs ≥ 0.917) (Fig S4 ,5). Significant associations with PFS were noted for DMNT3A, GNA11, IGF1, IRAK2, POLB, RAF1, THEM4, and XPA (Table S6, Fig S6-21).

RAF1 and XPA demonstrated significant hazard ratios 9.316 ($p = 0.042$) and 0.174 (Reciprocal HR: 5.732) ($p = 0.037$) (Fig S22-36, Table S7), respectively, indicating a strong association with disease progression. A correlation analysis revealed positive correlations between ALP ratios and BAX, PLCG2, and RAF1, while BDNF and TTK showed negative correlations (Table S8). Notably, in patients with non-progressive disease, a strong positive correlation ($r = 0.998$, $p = 0.037$) between ALP and GNA11 ratios was found, alongside a significant negative correlation with TTK ($r = -1.00$, $p = 0.009$) in patients responding to AL therapy (Table S9).

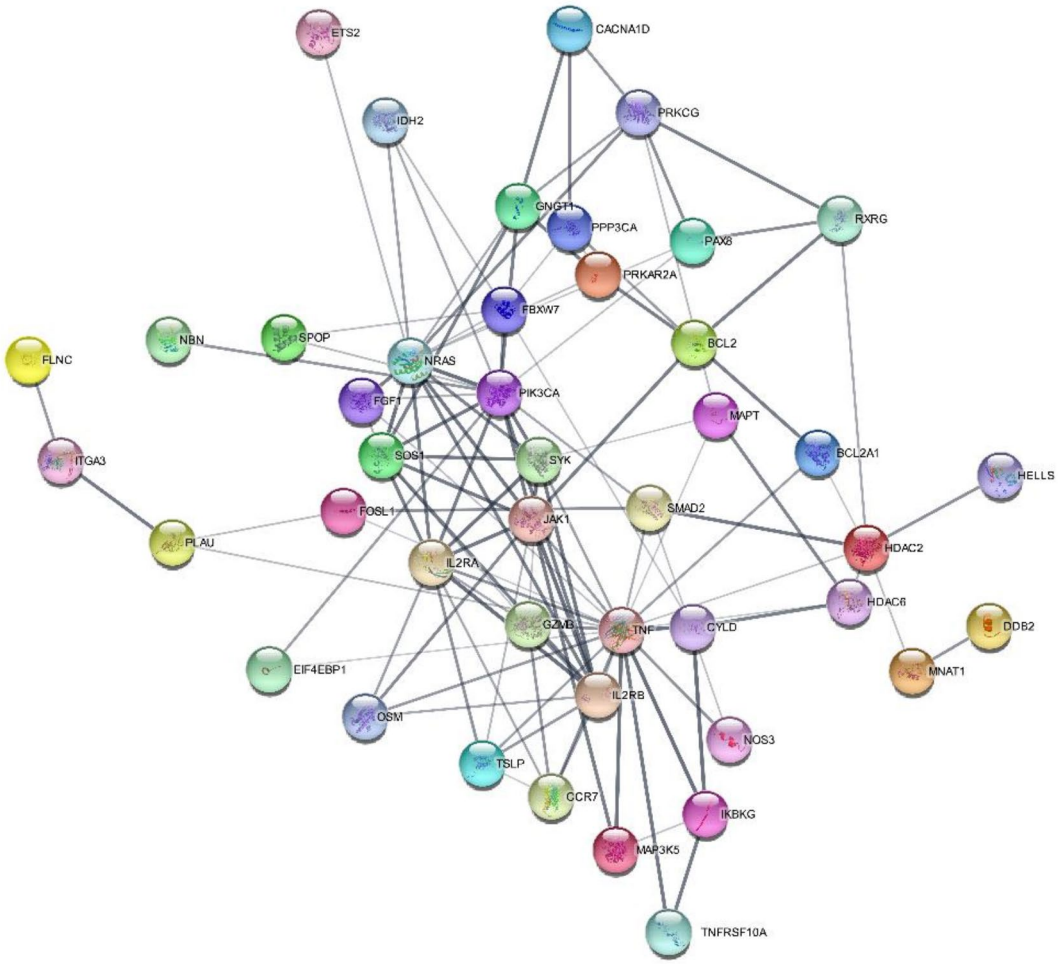

Fig. 2. A Molecular network of AL in patients with advanced-stage of intrahepatic cholangiocarcinoma (iCCA).

Survival status

No significant differences in known biomarkers were observed between survivors and non-survivors receiving AL therapy (p-values ranged from 0.145 to 1.00) (Table S10). ROC analysis revealed significant differences for AR and EYA1 ratios, both demonstrating AUC values of 1 ($p = 0.034$), with cut-off values of ≥ 1.895 and ≥ 1.67 folds, respectively (Fig S37, Table S11).

Significant differences in overall survival (OS) were observed for AR and EYA1 ($p = 0.008$) (Fig S38, 39, Table S12). The Cox hazard ratios did not demonstrate significant predictive value ($p = 0.504$) (Fig S40, 41, Table S13).

Strong positive correlations were found between AR and CA19-9 ratios (Table S14), and between EYA1 and CA19-9 ratios (Table S15), indicating a potential association of these biomarkers with survival outcomes. In addition, negative correlations were reported between AR and ALT ratios (Table S14), and between EYA1 and CPK ratios (Table S15, indicating an association of these biomarkers with survival outcomes.

Logistic regression highlighted RAF1 and XPA as significant predictors for disease progression, with acceptable McFadden's scores indicating model reliability.

Multi-logistic regression suggested that AR and EYA1 were significantly associated with OS, but the high McFadden's score indicated potential model inadequacy.

Probability risks for disease progression were stratified into four levels based on RAF1 and XPA ratios, suggesting tailored approaches for patient management based on risk assessment.

Adverse drug reactions

The incidence rates of grade 2 and 3 adverse events were consistent across groups, with no significant differences in blood parameters or liver function tests, suggesting minimal AL-related adverse effects.

Cross-talk among potential target genes and signaling pathways

Twenty-four enriched pathways were investigated for the interplay between the two functional interaction pathways. The cross-talk signaling pathways associated with tumor growth/proliferation/ survival of cancer, angiogenesis, and metastasis were categorized into three groups according to their abilities to depict the

Target	Degree	Betweenness	Closeness
TNF-α	22	765	0.57
PIK3CA	15	318	0.51
NRAS	14	236	0.47
JAK1	11	136	0.52
IL2RB	11	65.18	0.50
IL2RA	11	65.18	0.50
SYK	9	50.62	0.49
SOS1	9	27.88	0.43
HDAC2	7	286.72	0.46
GZMB	6	6.73	0.43
GNGT1	6	44.3	0.39
PRKCG	6	69.68	0.41
FBXW7	6	77.26	0.41
SMAD2	5	96.51	0.47
CCR7	5	0.5	0.42
BCL2	5	71.23	0.40
TSLP	5	1.06	0.42
PRKAR2A	4	14.56	0.36
RXRG	4	55.47	0.39
PAX8	4	20.13	0.39
OSM	4	0.0	0.42
PPP3CA	4	21.30	0.34
FGF1	4	25.96	0.46
CYLD	4	49.74	0.43
HDAC6	4	13.73	0.42
MAPT	4	49.19	0.44
IKBKG	4	5.36	0.39
PLAU	3	164	0.38
CAC1D	3	5.83	0.33
IDH2	3	0.0	0.36

Table 2. The major parameters of the top 30 targets in PPI networks in patients with advanced stage of intrahepatic cholangiocarcinoma (iCCA) after AL therapy.

mechanisms involved in tumor formation and invasion. The major cross-talk module consisted of various cellular processes, including cellular response to external stimuli, cell communication, regulation of cell death, signal transduction, and immune response.

Table 3 summarizes the cross-talk signaling pathways associated with tumor growth, proliferation, progression, survival, angiogenesis, and metastasis in patients with advanced-stage iCCA following AL therapy.

Tumor growth/proliferation/survival pathway The PI3K-AKT and JAK-STAT pathways demonstrated the highest similarity in tumor growth, proliferation, and survival, with a Jaccard value of 0.54, indicating significant overlap in the shared genes between the two pathways. The second-highest ranked pathways were MAPK-T cell receptor, NK-cell mediated toxicity-B cell receptor, Fc epsilon RI-proteoglycan, proteoglycan-T cell receptors, proteoglycan-NK-cell mediated cytotoxicity, PDL-1-Ras, PDL-1, and TNF-α signaling pathways.

Angiogenesis The highest-ranked pathways for angiogenesis included EGFR resistance-mTOR, EGFR resistance-Ras, EGFR resistance-PDL1, EGFR resistance-ErBb, ErBb-PDL1, ErBb-Ras, and ErBb-proteoglycan signaling, all showing the same level of similarity with a Jaccard index of 0.5, indicating significant cross-linking in their involvement.

Metastasis The regulation of actin cytoskeleton-Fc epsilon RI pathway had the highest Jaccard index for metastasis.

Candidate gene targets of AL

Gene targets associated with disease progression

Eleven gene targets and 18 edges, with an average degree of 3.27 [PPI], were used to build a comprehensive pharmacology-based network analysis in patients with progressive compared with non-progressive diseases. ERBB2 (1st rank), CDKN2A (2nd rank), BDNF (3rd rank), and IGF-1 (4th rank), DNMT3A (4th rank), Raf (4th rank) and GNA11 (4th rank) showed degrees of 8, 6, 4, 3, 3, 3, and 3, respectively, indicating their potential central hubs in regulating iCCA progression.

Three different analyses for regulating iCCA progression following functional analysis based on the eleven gene targets including KEGG pathway, biological processes, and Reactome pathway, were determined as follows:

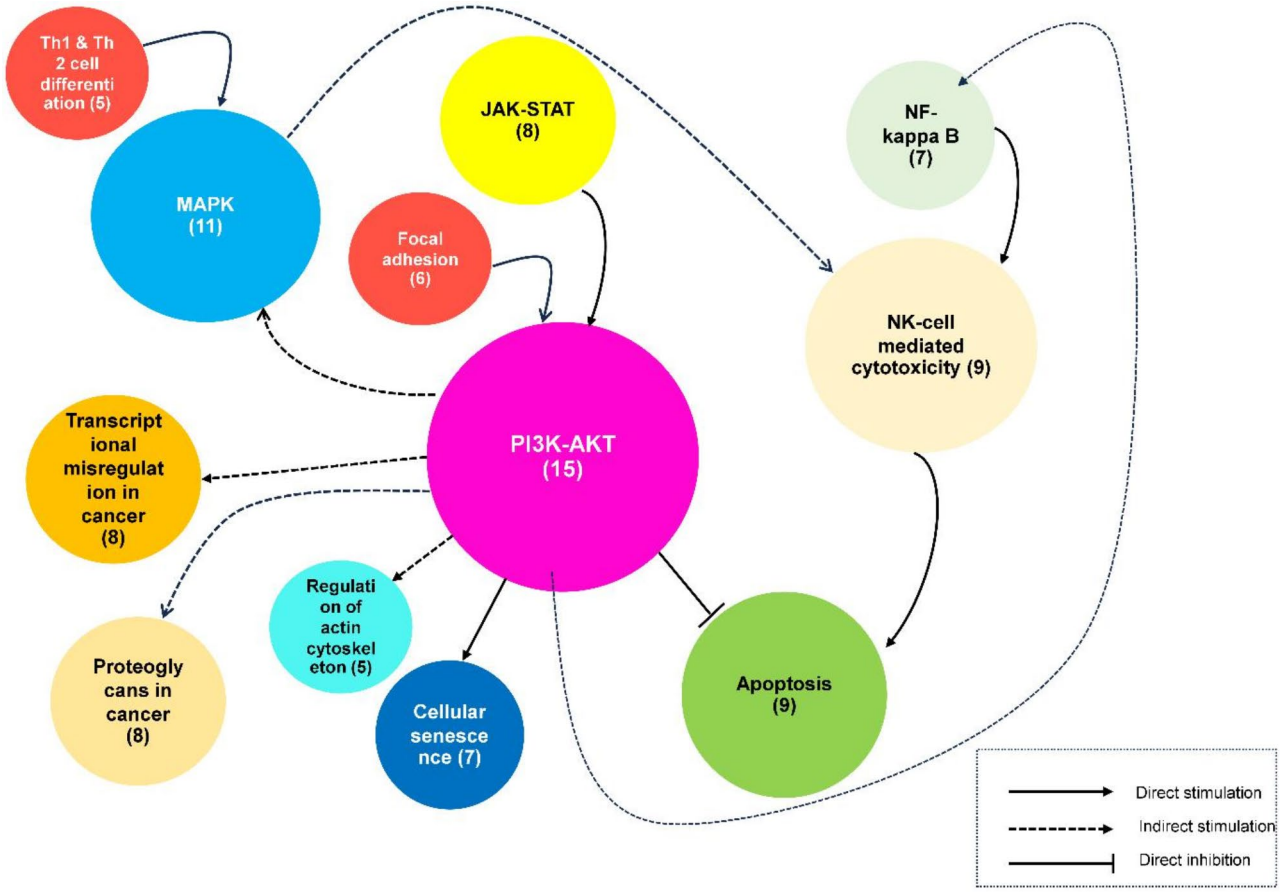

Fig. 3. The top 12 KEGG pathway in patients with advanced stage of intrahepatic cholangiocarcinoma after AL therapy.

i) KEGG analysis of the modulatory effects of AL on various signaling pathways such as the EGFR tyrosine kinase inhibitor, micro-RNA in cancer, Ras, TP53, platinum-drug resistance, MAPK, PI3K-AKT, ERBB2, and HIF-signaling pathways, II) signaling transduction of various biological processes, e.g., regulation of the cellular metabolic process and protein phosphorylation, and intracellular signal transduction, III) Reactome analysis of platelet activation and aggregation signaling pathways associated with GNA11, RAF1, IGF1, and PLCG2 target genes based on protein-protein interaction analysis.

Gene targets associated with survival
A comprehensive pharmacology-based network analysis was performed in survivors and non-survivors using seven gene targets and five edges, with an average degree [PPI] of 1.43. AR, FOS, HSPA1A, and MMP9 had degrees of 3 (1st rank), 3 (1st rank), 2 (2nd rank), and 2 (2nd rank). Functional enrichment analysis suggests that AL modulates toll-like receptor cascades, IL12 family signaling, regulation of mRNA stability, autophagy, signaling by NOTCH, regulation of TP53 activity, signaling by TGF-beta receptor complex, and MAPK family signaling cascades.

Binding affinity of AL to candidate gene targets
Table 4 summarizes the binding affinities of the three components of AL (atractylodin, beta-eudesmol, and atractylodin), standard drugs for iCCA (gemcitabine and 5-FU), and reference drugs/compounds (Ruxolitinib, idelalisib, panobinostat, SM16, GTP, BI-3406, Afatinib, and guadecitabine) to eleven candidate molecular targets of AL in iCCA. All reference drugs showed the highest binding affinities to all targets. Among the three components of AL, hinesol showed the highest binding affinities to all targets. The binding affinity of beta-eudesmol was relatively lower. Atractylodin weakly binds to most targets. For standard drugs, gemcitabine showed a high binding affinity comparable to hinesol. Residue proteins and root mean square deviation (RMSD) for each drug and target (binding affinity ≥ 6 kcal mol^{-1}) are shown in Supplementary figures S42-77.

Discussion

Associations between biomarkers and disease progression

This study identified an ALP ratio increase (≥ 1.024) as a potential predictor of iCCA progression following AL treatment. However, Kaplan-Meier analysis showed no significant correlation between ALP changes and

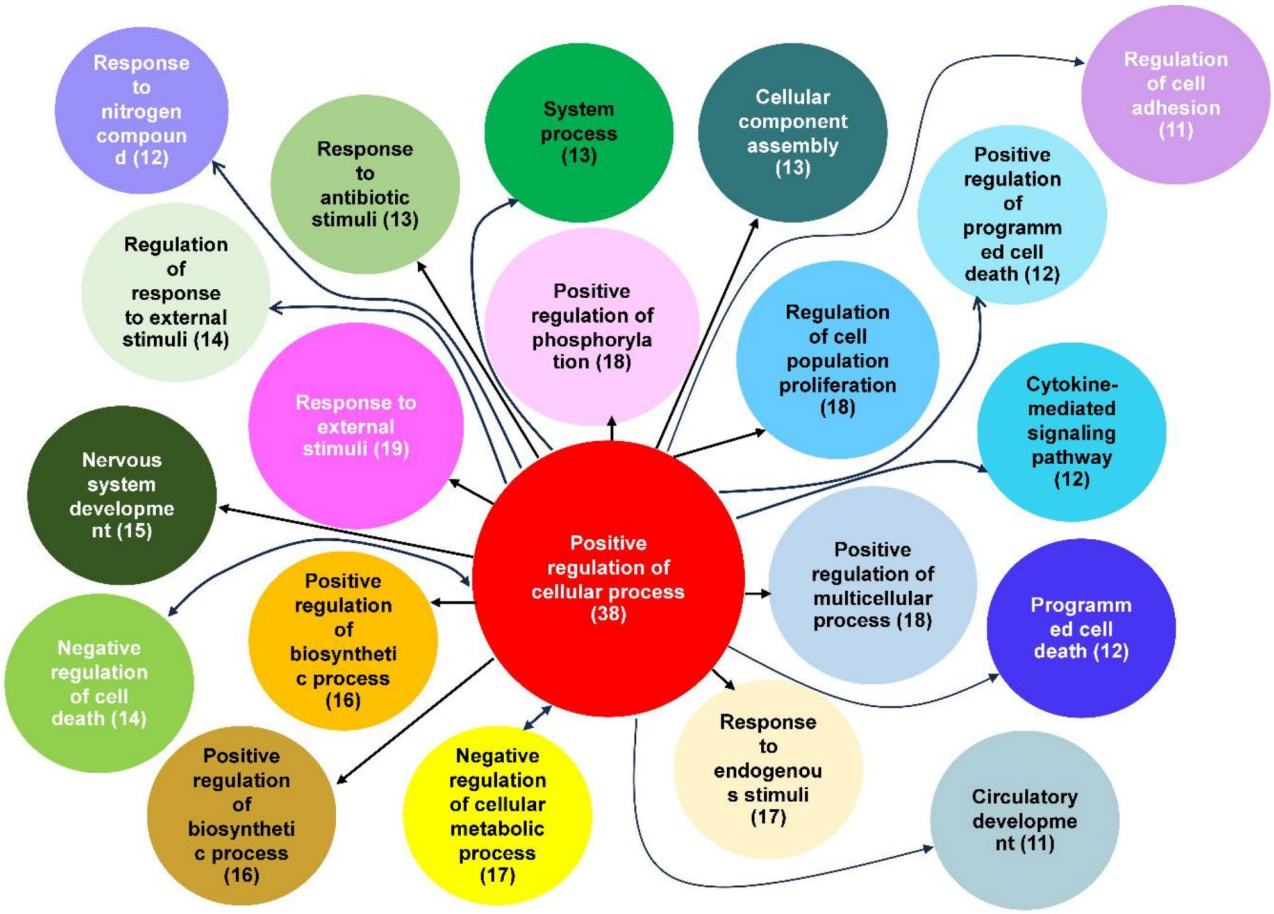

Fig. 4. The top 20 biological processes in patients with advanced stage of intrahepatic cholangiocarcinoma after AL.

progression-free survival (PFS), suggesting ALP ratios alone do not independently predict treatment response. Elevated ALP levels are linked to various hepatobiliary and metastatic conditions, including CCA, where high ALP correlates with rapid progression after gemcitabine-cisplatin treatment ($p = 0.01$)[14]. Additionally, high platelet counts and lower hemoglobin levels were associated with a worse prognosis, with hemoglobin showing a hazard ratio (HR) of 0.90 (95% CI = 0.83–0.97, $p = 0.009$)[15].

Regarding mRNA expression, 11 of 16 genes demonstrated predictive potential for AL response, with an area under the curve (AUC) > 0.9 ($p < 0.001$). Patients with RAF1 ratios ≥ 0.5 had a 9.32-fold higher risk of disease progression, while those with XPA levels < 1.34 had a 5.73-fold increased risk, emphasizing their role as early prognostic markers for AL therapy continuation. Elevated RAF1 ratios indicate heightened progression risk, whereas lower XPA levels suggest impaired DNA repair, contributing to disease advancement.

Unlike targeted mRNA/protein-based therapies, conventional chemotherapy (gemcitabine/cisplatin) lacks specific molecular targets. However, overexpression of ATP-binding cassette (ABC) transporters, such as ABCC1 (MRP1), reduces intracellular drug concentrations, contributing to 5-FU resistance[16]. Similarly, altered orotate phosphoribosyl transferase activity weakens FdUMP activation, impairing 5-FU efficacy, while OCT4 and MRP1 upregulation have been implicated in gemcitabine resistance[17]. Furthermore, FGFR2 alterations impact AKT/mTOR and STAT3 pathways, linking them to gemcitabine resistance, reinforcing the need for FGFR2 testing before treatment[18].

For targeted therapy, risk-stratified gene expression analysis identified HACL1, LAMA4, GMNN, C1RL, PCBD1, and FXYD2 as prognostic markers. The low-risk group responded better to bosutinib, gefitinib, gemcitabine, and paclitaxel, whereas the high-risk group showed improved responses to axitinib, cisplatin, and imatinib[19]. Additionally, PD-L1 expression serves as a prognostic indicator for immune checkpoint inhibitor (ICI) efficacy in iCCA patients. Notably, there was no overlap in the genetic markers associated with AL treatment and those linked to conventional or targeted therapies, suggesting distinct molecular pathways drive progressive disease under different therapeutic regimens.

Correlation analysis and prognostic markers

PLCG2 showed the strongest positive correlation with ALP ($r = 0.736$, $p = 0.01$), linking its activation of the ERK pathway to iCCA proliferation and apoptotic resistance. Patients with elevated PLCG2 levels experienced worse disease progression (1.40 vs. 0.41). Conversely, TTK, a promoter of tumor survival in gastric and hepatocellular

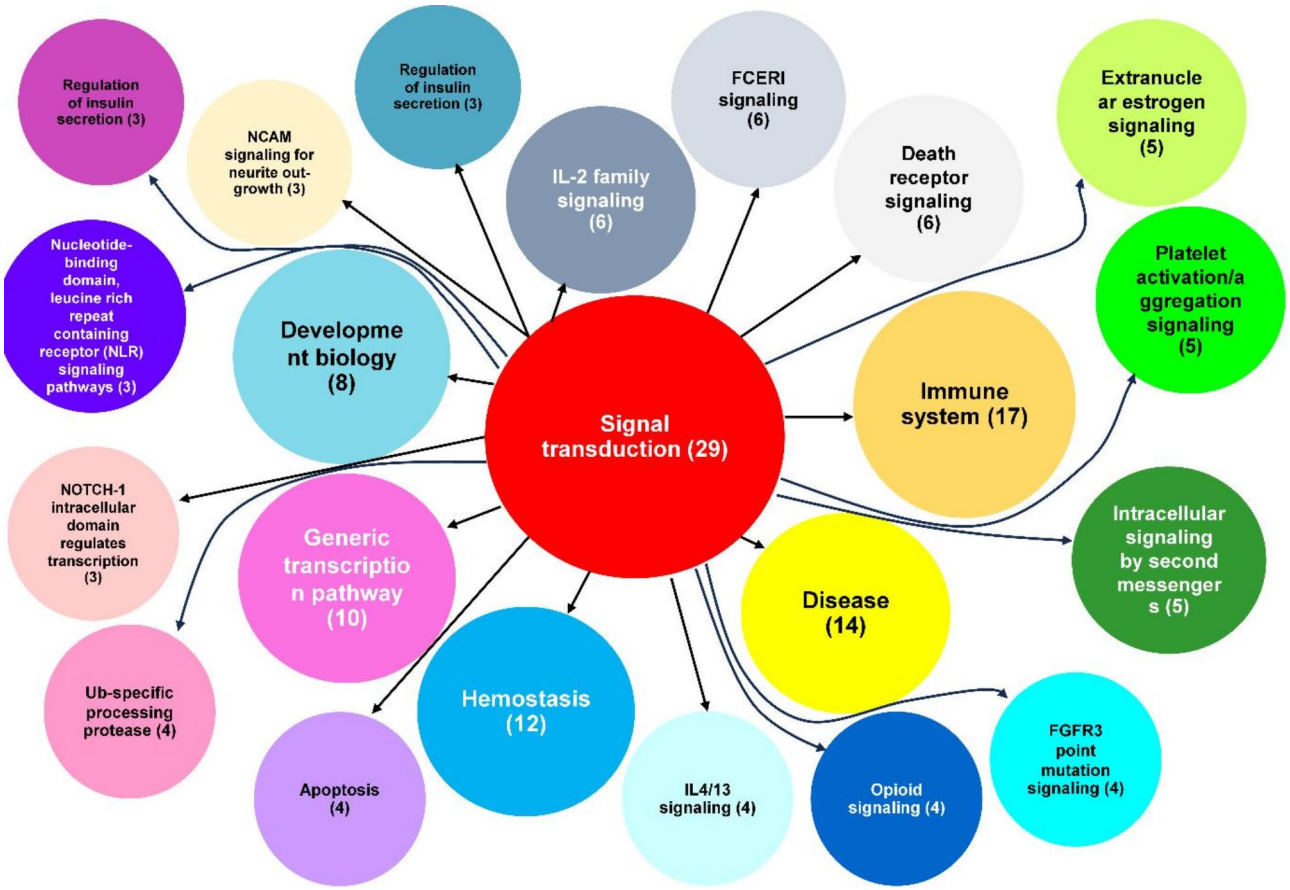

Fig. 5. The top 22 Reactome pathway in patients with advanced stage of intrahepatic cholangiocarcinoma after AL therapy.

cancers, exhibited a moderate inverse correlation with ALP (r=−0.727, p = 0.01). These findings suggest that genetic signatures play a role in cancer biomarker expression and disease progression.

RAF1 ratios correlated with increased progression risk, while lower XPA ratios indicated reduced risk. Raf-1 inhibition has been shown to suppress CCA metastasis by modulating MMP9/MMP4 expression and inhibiting EGF-induced cell growth[20]. Clinical studies reported an 18.1% partial response rate for Ras inhibitors across multiple cancers, including CCA[21]. Re-challenging Raf-1 inhibitors in BRAF-1 aberrant patients also yielded clinical responses, supporting its therapeutic potential.

XPA, crucial for nucleotide excision repair (NER), mediates platinum-based chemotherapy resistance[22]. In progressive iCCA cases, mRNA expression of XPA was elevated; however, XPA ratios < 1 suggest AL may suppress its expression, potentially reversing platinum resistance.

Combining AL with gemcitabine-cisplatin may enhance disease control rates (DCR) in patients with platinum-resistant iCCA compared to chemotherapy alone.

Survival analysis

This study found no significant differences in liver enzymes, CA19-9, CEA, or IL-6 between AL-treated iCCA patients and controls, suggesting these biomarkers may not predict survival in this cohort. However, the small sample size, with only two deaths recorded, may limit statistical power.

Previous studies have shown that ALP levels ≥ 138 IU/L were associated with shorter overall survival (HR = 1.654, 95% CI = 1.170–2.38, p = 0.004) following chemotherapy, compared to ALP < 138 IU/L (11.6 vs. 4.47 months)[23]. Similarly, CA19-9 < 1,000 IU/mL correlated with improved one-year survival[23]. While both gemcitabine and 5-FU influenced ALP levels, only gemcitabine-based treatment showed significant changes[23].

Jiang et al. reported that iCCA patients with ALP ≤ 147 IU/L had longer one-year and three-year survival (23 vs. 10.4 months) and a 1.64-fold higher probability of survival (95% CI = 1.20–2.22, p = 0.002) than those with ALP > 147 IU/L[24]. Higher CA19-9 levels were linked to better one-year survival than ALP ≤ 37 μg/mL (29.2 vs. 14.1 months), with a 1.80-fold increased survival probability (95% CI = 1.337–2.445, p < 0.001) in those with ALP ≤ 37 μg/mL[25].

These findings highlight the prognostic value of ALP and CA19-9 in iCCA, though their relevance in AL-treated patients remains unclear.

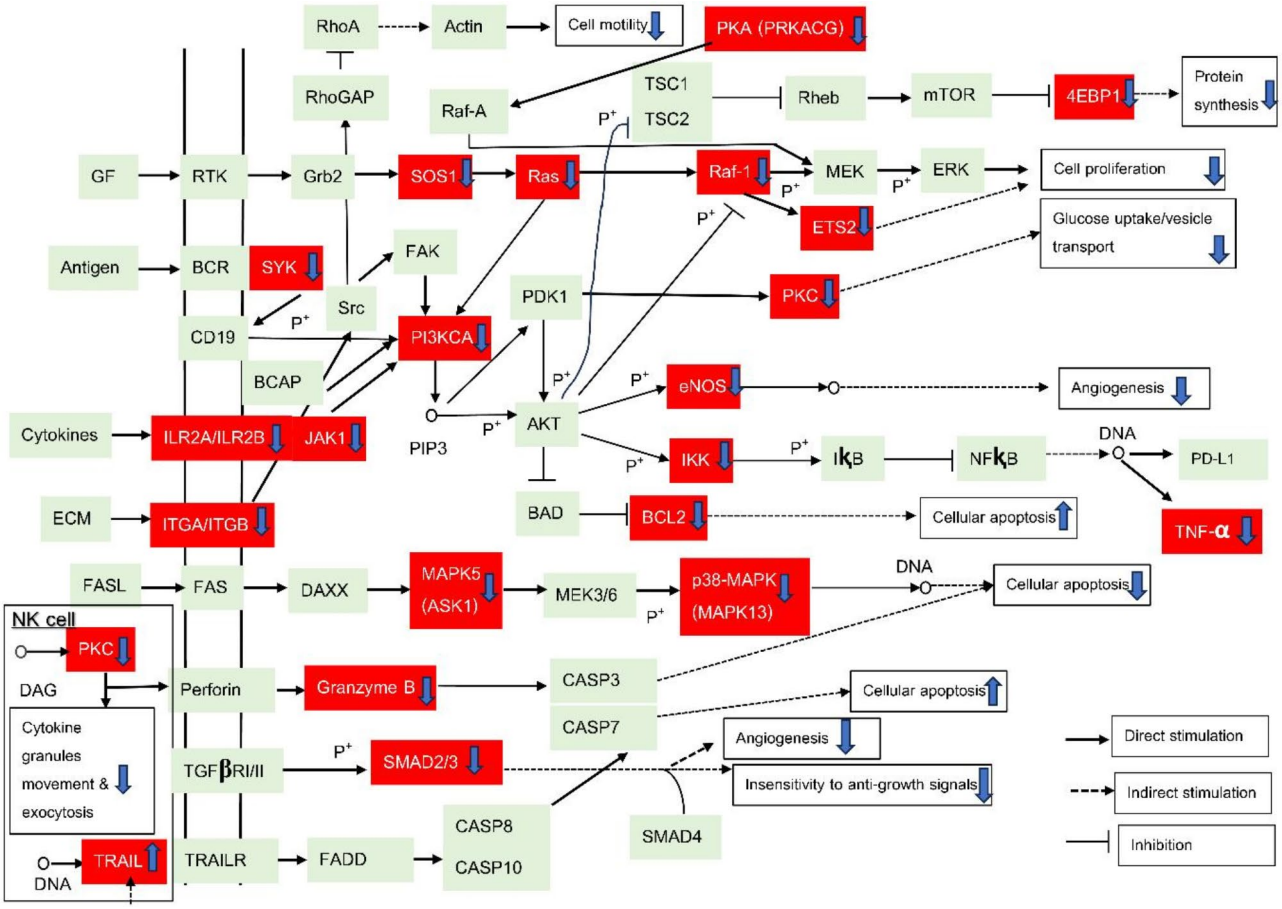

Fig. 6. A schematic diagram showing the proposed pharmacological mechanism of AL in patients with advanced-stage iCCA.

Promising candidate gene targets for AL

AL therapy targets critical pathways involved in iCCA progression, including PI3K-AKT, JAK-STAT, and Ras/MAPK/mTOR, which regulate tumor growth, survival, and immune evasion[26–34]. AL enhances immune response by stimulating NK, T-, and B-cell activity through genes such as GZMB, TNFRSF10A, PRKCG, PIK3CA, and SYK, which are linked to NK cell-mediated cytotoxicity and adaptive immunity[35–40].

Downregulation of tumor-promoting genes, including GNA11 (3.5-fold), IGF1 (7.2-fold), THEM4 (13.15-fold), PLCG2 (8.2-fold), POLB (7.14-fold), and RAF1 (17.35-fold), correlates with reduced tumor proliferation, differentiation, invasion, and metastasis[41–45]. Suppressing RAF1 may limit EGFR resistance and enhance the efficacy of EGFR/PI3K inhibitors, potentially overcoming drug resistance in iCCA[46–51]. Additionally, suppression of TSLP (7-fold), COL5A2, FLNC, ITGA3, and PLAU may improve overall survival by reducing tumor progression, angiogenesis, and immune suppression[52–57].

AL therapy appears to shift gene expression toward tumor suppression, supporting its potential as an adjunct treatment for advanced iCCA by inhibiting proliferation, reversing resistance, and enhancing immune response.

Proposed molecular targets of AL action

KEGG pathway enrichment analysis identified six critical pathways involved in iCCA progression following AL therapy: tumor proliferation, growth, survival, angiogenesis, invasion, and metastasis. The PI3K/AKT pathway (FDR = 2.26E-23) was the most significantly altered, impacting tumor progression through mTOR, Raf-1, NF-κB, MDM2, PDK1, p21/p27, Caspase 3/7/9, FOXO, eNOS, and MMP-2/9/13[17,18,34,41–45,53–82].

AL therapy modulated 15 key genes linked to the PI3K/AKT pathway, including OSM, SOS1, IL2RA, IL2RB, NRAS, NOS3, EIF4EBP1, JAK1, SYK, BCL-2, FGF1, IKBKG, ITGA3, GNGT1, and PIK3CA. Notably, JAK1 (33-fold downregulated) regulates tumor growth and immune response, and its suppression may control iCCA progression and reduce immunosuppressive effects[17,31,54,70–74]. OSM (downregulated), associated with lymphatic and distant metastasis, correlates with better overall survival (OS) and recurrence-free survival (RFS)[54]. NOS3 (downregulated) suppresses apoptosis and promotes angiogenesis via VEGF; its downregulation may inhibit metastasis[43,76]. EIF4EBP1 (downregulated) is linked to poor differentiation and lymph node metastasis in hilar CCA, and suppression may reduce tumor invasion[28]. SOS1 (22-fold downregulated) regulates PI3K/AKT, EMT, and MAPK signaling, and its suppression could inhibit EGFR resistance, EMT, and metastasis[78–80]. ITGA3 (8-fold downregulated) activates PI3K through focal adhesion; downregulation correlates with reduced tumor size,

Pathway A	Pathway B	Jaccard index
Growth/proliferation/survival tumor		
PI3K-AKT	JAK-STAT	0.54
MAPK	T cell receptor	0.5
NK-cell mediated cytotoxicity	B cell receptor	0.5
Fc epsilon	Proteoglycan	0.5
Proteoglycan	T-cell receptor	0.5
Proteoglycan	NK-cell mediated cytotoxicity	0.5
NK-cell mediated cytotoxicity	Proteoglycan	0.5
PDL-1	Ras	0.5
PDL-1	TNF-alpha	0.5
NK-cell mediated cytotoxicity	T-cell receptor	0.44
APOPTOSIS	TNF-alpha	0.43
mTOR	Proteoglycan	0.43
Proteoglycan	Ras	0.43
MAPK	B cell receptor	0.4
APOPTOSIS	NF-Kappa	0.4
MAPK	NK-cell mediated cytotoxicity	0.38
JAK-STAT	mTOR	0.38
mTOR	NK-cell mediated cytotoxicity	0.38
Proteoglycan	B cell receptor	0.38
mTOR	T-cell receptor	0.33
Proteoglycan	Cell senescence	0.33
MAPK	Apoptosis	0.31
MAPK	Proteoglycan	0.31
MAPK	mTOR	0.3
MAPK	Ras	0.3
MAPK	PDL-1	0.3
MAPK	TNF-alpha	0.3
MAPK	RIG-I like receptor	0.3
Proteoglycan	Focal adhesion	0.3
Proteoglycan	APOPTOSIS	0.27
PI3K-AKT	mTOR	0.25
PI3K-AKT	Ras	0.25
JAK-STAT	PDL-1	0.25
Apoptosis	P53 signaling	0.25
Apoptosis	RIG-I like receptor	0.25
Apoptosis	Platinum drug resistance	0.25
NF-kappa	TNF-alpha	0.25
NF-kappa	RIG-I like receptor	0.25
Proteoglycan	PDL-1	0.25
Proteoglycan	TNF-signaling	0.25
Apoptosis	NK-cell mediated cytotoxicity	0.25
Angiogenesis		
EGFR-resistance	PI3K-AKT	0.5
EGFR-resistance	mTOR	0.5
EGFR-resistance	Ras	0.5
EGFR-resistance	PDL-1	0.5
EGFR-resistance	ErBb signaling	0.5
ErBb signaling	PDL-1	0.5
ErBb signaling	Ras	0.5
ErBb signaling	Proteoglycan	0.5
EGFR-resistance	B-cell receptor	0.43
ErBb signaling	Regulation of actin cytoskeleton	0.4
EGFR-resistance	JAK-STAT	0.4
ErBb signaling	B-cell receptor	0.4
EGFR-resistance	Fc epsilon	0.38
Continued		

Pathway A	Pathway B	Jaccard index
EGFR-resistance	T-cell receptor	0.38
ErBb signaling	Fc epsilon	0.33
ErBb signaling	T-cell receptor	0.33
EGFR-resistance	Proteoglycan	0.3
EGFR-resistance	Platinum resistance	0.28
EGFR-resistance	NK-cell mediated cytotoxicity	0.27
ErBb signaling	PI3K-AKT	0.25
Metastasis		
Regulation of actin cytoskeleton	T-Cell receptor	0.5
Regulation of actin cytoskeleton	Fc epsilon	0.5
Regulation of actin cytoskeleton	EGFR-resistance signaling	0.43
Regulation of actin cytoskeleton	VEGFR signaling	0.4
Regulation of actin cytoskeleton	PDL-1	0.4
Regulation of actin cytoskeleton	Proteoglycan	0.38
Regulation of actin cytoskeleton	PI3K-AKT	0.33
Regulation of actin cytoskeleton	NK-cell mediated cytotoxicity	0.33
Regulation of actin cytoskeleton	MAPK	0.27

Table 3. A cross-talk pathway between the different pathways.

lymph node metastasis, and advanced TNM stage[56]. BCL-2 (7-fold downregulated) is linked to chemoresistance, and its suppression may enhance apoptosis and treatment response[46,75]. FGF1 (14-fold upregulated) potentially activates angiogenesis via PI3K/AKT, although its impact may be minimal due to low FGFR1 overexpression in iCCA[83–85].

Downregulation of key oncogenic genes in the PI3K/AKT pathway suggests that AL therapy suppresses iCCA proliferation, growth, angiogenesis, and metastasis. The 6-fold downregulation of PIK3CA indicates a significant reduction in pathway activation, supporting the observed improvements in OS and progression-free survival (PFS) in AL-treated patients compared to palliative care. These findings position AL as a promising adjunct therapy in advanced-stage iCCA.

NK cell-mediated cytotoxicity

The NK cell-mediated cytotoxicity pathway was the second most altered pathway following AL therapy, involving key immune response regulators like GZMB, TNFRSF10A, TNF-α, PKCG, and PIK3CA[84]. GZMB (downregulated) is essential for apoptosis via caspase-3/7 activation, and its reduction may impair NK and T-cell cytotoxicity, affecting immunosuppressive functions[52]. TNFRSF10A (10-fold upregulated), also known as TRAIL-1, promotes apoptosis in iCCA cells through DR4/5 activation. Its increase may compensate for GZMB downregulation, enhancing tumor cell death[29]. TNF-α (downregulated) plays a role in NK cell proliferation and cytotoxicity, but its reduction did not significantly affect CDKN2A expression, indicating stable NK cell function[80,81].

AL therapy modulates NK cell-mediated immune responses, potentially suppressing granzyme-mediated apoptosis while enhancing TRAIL-dependent apoptosis, supporting its anti-tumor effects in iCCA. Additionally, downregulation of key oncogenic genes in the PI3K/AKT pathway suggests AL therapy inhibits iCCA proliferation, growth, angiogenesis, and metastasis. Notably, the 6-fold downregulation of PIK3CA indicates a significant reduction in pathway activation, supporting the observed improvements in OS and PFS in AL-treated patients compared to palliative care. These findings position AL as a promising adjunct therapy for advanced-stage iCCA.

Apoptosis pathway

The apoptosis pathway ranked third among the pathways linked to AL action, involving genes such as GZMB, TNFRSF10A, PI3KCA, BCL-2A1, MAP3K5, NRAS, BCL-2, TNF, and IKBKG. BCL-2A1, an anti-apoptotic protein, promotes survival in various cancers, with higher overexpression in lymphoma and leukemia patients compared to those with solid tumors[86]. In advanced-stage solid tumors, BCL-2A1 upregulation is linked to chemoresistance[86]. The downregulation of both BCL-2A1 and BCL-2 after AL therapy may increase sensitivity to chemotherapy-resistant iCCA.

In silico docking simulation

In silico docking results revealed high binding affinities of hinesol and beta-eudesmol to the candidate molecular targets, supporting AL's clinical efficacy in a phase IIA trial[12]. While hinesol showed low cytotoxic potency against iCCA cells[87], it had high binding affinity to all targets except HDAC2, NRAS, and SOS1. Notably, hinesol combined with beta-eudesmol or atractylodin exhibited synergistic cytotoxic effects across all iCCA cell lines[87]. These findings suggest that the compounds effectively bind to their molecular targets, preventing tumor development and inducing cell death. Gemcitabine demonstrated higher binding affinity than 5-FU to all targets, likely due to the differing molecular targets of the two drugs—5-FU targets thymidylate synthase, while

Protein target	Drug/compound	Binding affinity (kcal mol^{-1})
JAK1	Ruxolitinib (standard JAK1 inhibitor)	−7.5
	β-eudesmol	−7.04
	Atractylodin	−5.58
	Hinesol	−7.62
	5-FU	−4.1
	Gemcitabine	−5.95
PI3KCA	Idelalisib (standard PI3KCA inhibitor)	−7.69
	β-eudesmol	−7.27
	Atractylodin	−5.7
	Hinesol	−8.76
	5-FU	−4.55
	Gemcitabine	−6.41
HDAC2	Panobinostat	−9.9
	β-eudesmol	−6.73
	Atractylodin	−5.87
	Hinesol	−8.55
	5-FU	−3.88
	Gemcitabine	−5.6
IL2RA	β-eudesmol	−6.34
	Atractylodin	−4.8
	Hinesol	−7.3
	5-FU	−3.24
	Gemcitabine	−6.19
IL2RB	β-eudesmol	−6.43
	Atractylodin	−5.11
	Hinesol	−7.3
	5-FU	−3.45
	Gemcitabine	−5.1
TNF-α	β-eudesmol	−5.45
	Atractylodin	−3.67
	Hinesol	−6.01
	5-FU	−3.15
	Gemcitabine	−4.35
SMAD2	SM16 (standard SMAD2 inhibitor)	−7.88
	β-eudesmol	−7.56
	Atractylodin	−1.44
	Hinesol	−9.02
	5-FU	−3.84
	Gemcitabine	−6.02
NRAS	GTP (standard NRAS inhibitor)	−8.9
	β-eudesmol	−7.59
	Atractylodin	−5.3
	Hinesol	−7.99
	5-FU	−4.63
	Gemcitabine	−7.24
SOS1	BI-3406 (standard SOS1 inhibitor)	−8.3
	β-eudesmol	−7.41
	Atractylodin	−5.7
	Hinesol	−7.74
	5-FU	−3.63
	Gemcitabine	−6.00
Continued		

Protein target	Drug/compound	Binding affinity (kcal mol^{-1})
ERBB2	Afatinib (standard ERBB2 inhibitor)	−7.37
	β-eudesmol	−6.66
	Atractylodin	−4.44
	Hinesol	−6.8
	5-FU	−4.54
	Gemcitabine	−6.22
DNMT3A	Guadecitabine (standard DNMT3A)	−12.92
	β-eudesmol	−7.67
	Atractylodin	−6.05
	Hinesol	−8.51
	5-FU	−4.47
	Gemcitabine	−7.01

Table 4. The binding affinities of the three components of AL (atractylodin, b-eudesmol, and atractylodin), standard drugs for iCCA (gemcitabine and 5-FU), and reference drugs/compounds (Ruxolitinib, idelalisib, Panobinostat, SM16, GTP, BI-3406, Afatinib, and guadecitabine) to eleven candidate molecular targets of AL in iCCA.

gemcitabine targets DNA replication components[88]. Patients treated with gemcitabine plus cisplatin[89]showed superior tumor control, time-to-progression, disease-free survival, and overall survival compared to those treated with 5-FU, leucovorin, and cisplatin[89]. 5-FU and gemcitabine were selected for docking simulation as first-line treatments for intrahepatic cholangiocarcinoma, although their mechanisms of action are limited to targeting AL-related molecules such as JAK1, PI3KCA, HDAC2, and IL2RA. Further preclinical studies are needed to confirm the efficacy of gemcitabine and 5-FU on these potential targets.

Potential errors and bias

Potential errors in ligand-receptor interactions affecting ligand binding affinity can be categorized into four sources as follows:

Protein structure Missing residues or domains may alter the binding pocket geometry. Incorrect rotamer assignments within the binding pocket can misalign interactions with the ligand. Protein flexibility is often overlooked.

Ligand Inadequate sampling of ligand conformations may underestimate the optimal binding pose. Incorrect protonation states of functional groups can affect receptor interactions. Inaccurate force field parameters can lead to incorrect energy calculations.

Docking algorithm Search algorithms may fail to sufficiently sample potential binding modes, especially in complex interactions. Improperly defined binding sites may lead to irrelevant biological targets.

Environmental factors Not accounting for water molecules around the binding site can distort protein-ligand interaction.

Evidence before this study

Beta-eudesmol, atractylodin, and hinesol --key active compounds of *Atractylodes lancea*(Thunb) DC exhibit antiproliferative, apoptotic, anti-metastatic, and anti-angiogenic effects through multiple mechanisms: (i) promotion of cell cycle arrest through modulation of p16, CDK1, CDK4, and p21[8]; (ii) apoptosis activation through increasing Bax/Bcl2 ratio, TNFRSF6, cytochrome C, and caspase activation (caspase-3, −8, −9, Apaf1, Bax-3)[8,90]; (iii) immunostimulation through enhancing CDKN2B expression, promoting immune control of iCCA[90]; (iv) PI3K-AKT pathway suppression through downregulating phosphorylated PI3K, AKT, p-p38MAPK, STAT1/3, HO1, and NF-κB[6,91]; (v) anti-angiogenesis through downregulating Vegfa and Vegfr2 expression[7]; and (vi) anti-metastatic effects through downregulating MMP9, N-Cadherin, and TGF-beta expression[8].

These findings stem from in vitro and in vivo studies; however, clinical validation in humans remains lacking.

Added value of this study

This is the first study to provide a network analysis of AL and its bioactive constituents—beta-eudesmol, atractylodin, and hinesol—in patients with advanced intrahepatic cholangiocarcinoma (iCCA). Our findings demonstrate that AL inhibits iCCA growth through multiple mechanisms. AL promotes apoptosis via Bcl-2, Bcl-2A1, ASK, and SMAD2, enhances NK cell-mediated cytotoxicity through FAS-TRAIL, TNFRSF10A, PKCG, and TNF-alpha, and suppresses CCA metastasis by targeting ITGA3 and EIF4EBP1. It also affects angiogenesis by interacting with NOS3, ERBB2, and FGF1/FGFR1. Additionally, AL sensitizes CCA to gemcitabine/5-FU-induced chemoresistance by modulating the Bcl-2/Bcl-2A1 pathway. Docking simulations confirm that AL bioactives bind to key targets, including JAK-1, HDAC2, IL2RA, SMAD2, NRAS, SOS1, ERBB2, and DNMT3A, which are involved in metastasis and angiogenesis. Notably, RAF1 and XPA were identified as potential new targets for CCA therapies.

Implications of all the available evidence

Our data, consistent with previous studies, show that AL and its bioactive compounds significantly control cholangiocarcinoma (CCA) through multiple mechanisms, including enhancing apoptosis, inhibiting cellular growth, boosting NK cell-mediated cytotoxicity, preventing angiogenesis, and inhibiting invasion. We also identify new targeted proteins for CCA therapy. Previous research highlights AL's antiproliferative effects, mainly via the PI3K/AKT pathway, and its role in caspase-dependent and independent apoptosis, anti-angiogenesis, and tumor invasion prevention. Through network analysis, we identified new targets and confirmed existing ones. Notably, patients treated with AL and exhibiting non-progressive disease (with lower RAF1 and higher XPA expressions) provide valuable insights for developing new drugs and treatment strategies for intrahepatic cholangiocarcinoma (iCCA).

Impacts of the study

Combining AL with a first-line regimen (gemcitabine plus cisplatin) may improve the disease control rate (DCR) in patients with platinum-based chemotherapy resistance. This study's results, using a probability approach, serve as early prognostic markers, aiding in predicting the DCR, minimizing unnecessary treatments, and maximizing efficacy in clinical settings.

Limitations

The statistical analysis of multiple comparisons may be limited by a false positive rate, as Bonferroni correction was not applied. Additionally, the molecular network relies on static protein-protein interactions (PPI), while PPIs are dynamic, and gene expression can change over time. mRNA expression may not always correlate with protein translation, and further validation through protein expression, proteomics, and functional analysis, including western blot and kinetic binding assays, is needed to confirm these results.

While docking simulations provide useful insights into protein-ligand binding affinity, their accuracy is influenced by the quality of input data (protein structure, ligand quality, docking algorithm, and environmental factors). Neglecting protein flexibility, as seen with AutoDock Vina, may lead to inaccurate binding affinity calculations. Further assays, including western blot analysis and kinetic binding studies, are necessary to validate the interactions between AL bioactives and their targets. The Lamarckian Genetic Algorithm (LGA) in AutoDock accounts for flexible ligand poses, helping predict binding affinity for flexible proteins in biological contexts. However, limitations like atom type constraints and memory issues can result in long computational times. These limitations can be minimized by using well-refined protein structures (from X-ray crystallography or NMR with ≤ 3 Å resolution), selecting complete protein residues, defining binding pockets based on existing literature, and considering the role of surrounding water molecules.

Conclusion

A molecular networking study confirmed AL as a potential alternative treatment for iCCA by targeting key pathways such as PI3K/AKT, NK cell-mediated cytotoxicity, and apoptosis. These pathways regulate iCCA development, progression, angiogenesis, and invasion. This study highlights the utility of molecular networking in identifying signaling targets of herbal medicines, which contain both active and non-active components.

Data availability

The authors confirm that the data supporting the findings of this study are available within the article and/or its Supplementary Materials and Methods. The datasets used and/or analysed during the current study are available from the corresponding author upon reasonable request.

Received: 10 May 2024; Accepted: 24 February 2025
Published online: 10 May 2025

References

1. Banales, J. M. et al. Cholangiocarcinoma 2020: The next horizon in mechanisms and management. *Nat. Rev. Gastroenterol. Hepatol.* **17:9**, 557–588. https://doi.org/10.1038/s41575-020-0310-z (2020). Epub 2020 Jun 30.
2. Na-Bangchang, K., Plengsuriyakarn, T. & Karbwang, J. Research and development of atractylodes lancea (Thunb) DC. as a promising candidate for cholangiocarcinoma chemotherapeutics. *Evid. Based Complement. Alternat Med.* **2017**, 5929234. https://doi.org/10.1155/2017/5929234 (2017).
3. Martviset, P., Chaijaroenkul, W., Muhamad, P. & Na-Bangchang, K. Bioactive constituents isolated from *Atractylodes lancea* (Thunb.) DC. rhizome exhibit synergistic effect against cholangiocarcinoma cell. *J. Exp. Pharmacol.* **10**, 59–64 (2018).
4. Kotawong, K., Chaijaroenkul, W., Muhamad, P. & Na-Bangchang, K. Cytotoxic activities and effects of atractylodin and β-eudesmol on the cell cycle arrest and apoptosis on cholangiocarcinoma cell line. *J. Pharmacol. Sci.* **136**(2), 51–56. https://doi.org/10.1016/j.jphs.2017.09.033 (2018).
5. Srijiwangsa, P., Ponnikorn, S. & Na-Bangchang, K. Effect of β-eudesmol on NQO1 suppression-enhanced sensitivity of cholangiocarcinoma cells to chemotherapeutic agents. *BMC Pharmacol. Toxicol.* **19**(1), 32. https://doi.org/10.1186/s40360-018-0223-4 (2018).
6. Acharya, B., Chajaroenkul, W. & Na-Bangchang, K. β-Eudesmol inhibits the migration of cholangiocarcinoma cells by suppressing epithelial-mesenchymal transition via PI3K/AKT and p38MAPK modulation. *Asian Pac. J. Cancer Prev.* **23** (8), 2573–2581. https://doi.org/10.31557/APJCP.2022.23.8.2573 (2022).
7. Tshering, G., Pimtong, W., Plengsuriyakarn, T. & Na-Bangchang, K. Anti-angiogenic effects of beta-eudesmol and atractylodin in developing zebrafish embryos. *Comp. Biochem. Physiol. C Toxicol. Pharmacol.* **243**, 108980. https://doi.org/10.1016/j.cbpc.2021.108980 (2021).
8. Sonsomnuek, P., Tarasuk, M., Plengsuriyakarn, T., Boonprasert, K. & Na-Bangchang, K. Apoptotic and anti-metastatic effects of *Atractylodes lancea* (Thunb.) DC. in a Hamster model of cholangiocarcinoma. *Asian Pac. J. Cancer Prev.* **23** (9), 3093–3101. https://doi.org/10.31557/APJCP.2022.23.9.3093 (2022).

9. Zuo, J. et al. Integrating molecular network and metabolomics study on anti-rheumatic mechanisms and antagonistic effects against methotrexate-induced toxicity of Qing-Luo-Yin. *Front. Pharmacol.* **9**, 1472. https://doi.org/10.3389/fphar.2018.01472 (2018). [old: 5].
10. Liu, Z., Ma, H. & Lai, Z. Revealing the potential mechanism of *Astragalus membranaceus* improving prognosis of hepatocellular carcinoma by combining transcriptomics and molecular network. *BMC Complement. Med. Ther.* **21**(1), 263. https://doi.org/10.1186/s12906-021-03425-9 (2021).
11. Lu, Y., Dong, K., Yang, M. & Liu, J. Molecular network-based strategy to investigate the bioactive ingredients and molecular mechanism of *Evodia rutaecarpa* in colorectal cancer. *BMC Complement. Med. Ther.* **23**, 1433. https://doi.org/10.1186/s12906-023-04254-8 (2023).
12. Na-Bangchang, K. et al. Phase IIa clinical trial to evaluate safety and efficacy of capsule formulation of the standardized extract of *Atractylodes lancea* (Thunb) DC in patients with advanced-stage intrahepatic cholangiocarcinoma. *J. Tradit Complement. Med.* (2023). (In press).
13. Odongo, R., Demiroglu-Zergeroglu, A. & Çakır, T. A systems pharmacology approach based on oncogenic signalling pathways to determine the mechanisms of action of natural products in breast cancer from transcriptome data. *BMC Complement. Med. Ther.* **21**(1), 181. https://doi.org/10.1186/s12906-021-03340-z (2021).
14. Zhou, Z. et al. Tumor-associated neutrophils and macrophages interaction contributes to intrahepatic cholangiocarcinoma progression by activating STAT3. *J. Immunother Cancer* **9**(3), e001946. https://doi.org/10.1136/jitc-2020-001946 (2021).
15. Yothaisong, S. et al. Increased activation of PI3K/AKT signaling pathway is associated with cholangiocarcinoma metastasis and PI3K/mTOR Inhibition presents a possible therapeutic strategy. *Tumour Biol.* **34**(6), 3637–3648. https://doi.org/10.1007/s13277-013-0945-2 (2013).
16. Fang, Z., Lu, L., Tian, Z. & Luo, K. Overexpression of phosphorylated 4E-binding protein 1 predicts lymph node metastasis and poor prognosis of Chinese patients with hilar cholangiocarcinoma. *Med. Oncol.* **31**, 5940. https://doi.org/10.1007/s12032-014-0940-5 (2014).
17. Liao, W., Lin, J. X. & Leonard, W. J. Interleukin-2 at the crossroads of effector responses, tolerance, and immunotherapy. *Immunity* **38**(1), 13–25. https://doi.org/10.1016/j.immuni.2013.01.004 (2013).
18. Biswas, P. et al. Analysis of SYK gene as a prognostic biomarker and suggested potential bioactive phytochemicals as an alternative therapeutic option for colorectal cancer: an in-silico pharmaco-Informatics investigation. *J. Pers. Med.* **11** (9), 888. https://doi.org/10.3390/jpm11090888 (2021).
19. Kang, Q. et al. Characterization and prognostic significance of mortalin, Bcl-2 and Bax in intrahepatic cholangiocarcinoma. *Oncol. Lett.* **15**, 2161–2168. https://doi.org/10.3892/ol.2017.7570 (2018).
20. Chen, L. & Tiannqianng, S. Multi-omics characterization of cholangiocarcinoma and association with prognostic and therapeutic molecular subtypes (abstract). *ASCO* Supplemennt_1.60 (2023)
21. Xia, T. et al. Immune cell atlas of cholangiocarcinomas reveals distinct tumor microenvironments and associated prognoses. *J. Hematol. Oncol.* **15**(1), 37. https://doi.org/10.1186/s13045-022-01253-z (2022).
22. Taniai, M. et al. Mcl-1 mediates tumor necrosis factor-related apoptosis-inducing ligand resistance in human cholangiocarcinoma cells. *Cancer Res.* **64**(10), 3517–3524. https://doi.org/10.1158/0008-5472.CAN-03-2770 (2004).
23. Kobayashi, S., Werneburg, N. W., Bronk, S. F., Kaufmann, S. H. & Gores, G. J. Interleukin-6 contributes to Mcl-1 up-regulation and TRAIL resistance via an Akt-signaling pathway in cholangiocarcinoma cells. *Gastroenterology* **128**(7), 2054–2065. https://doi.org/10.1053/j.gastro.2005.03.010 (2005).
24. Roy, S., Glaser, S. & Chakraborty, S. Inflammation and progression of cholangiocarcinoma: Role of angiogenic and lymphangiogenic mechanisms. *Front. Med. (Lausanne)* **6**, 293. https://doi.org/10.3389/fmed.2019.00293 (2019).
25. Ma, L. et al. Single-cell atlas of tumor cell evolution in response to therapy in hepatocellular carcinoma and intrahepatic cholangiocarcinoma. *J. Hepatol.* **75**, 1397–1408. https://doi.org/10.1016/j.jhep.2021.06.028 (2021).
26. Vogler, M. BCL2A1: The underdog in the BCL2 family. *Cell. Death Differ.* **19**, 67–74. https://doi.org/10.1038/cdd.2011.158 (2012).
27. Pan, J. et al. Reactive oxygen species-activated akt/ask1/p38 signaling pathway in nickel compound-induced apoptosis in Beas 2b cells. *Chem. Res. Toxicol.* **23**, 568–557 (2010).
28. Donato, N. J. & Perez, M. Tumor necrosis factor-induced apoptosis stimulates p53 accumulation and p21WAF1 proteolysis in ME-180 cells. *J. Biol. Chem.* **273**(9), 5067–5072. https://doi.org/10.1074/jbc.273.9.5067 (1998).
29. Gámez-García, A. et al. ERK5 Inhibition induces autophagy-mediated cancer cell death by activating ER stress. *Front. Cell. Dev. Biol.* **9**, 742049. https://doi.org/10.3389/fcell.2021.742049 (2021).
30. Stoyanova, T., Roy, N., Kopanja, D., Bagchi, S. & Raychaudhuri, P. DDB2 decides cell fate following DNA damage. *Proc. Natl. Acad. Sci. U S A.* **106**(26), 10690–10695. https://doi.org/10.1073/pnas.0812254106 (2009).
31. Prager, I. & Watzl, C. Mechanisms of natural killer cell-mediated cellular cytotoxicity. *J. Leukoc. Biol.* **105**(6), 1319–1329. https://doi.org/10.1002/JLB.MR0718-269R (2019).
32. Moon, T. D., Morley, J. E., Vessella, R. L. & Lange, P. H. The role of calmodulin in human natural killer cell activity. *Scand. J. Immunol.* **18**(3), 255–258. https://doi.org/10.1111/j.1365-3083.1983.tb00865.x (1983).
33. Yan, Y., Gao, Z., Han, H., Zhao, Y. & Zhang, Y. NRAS expression is associated with prognosis and tumor immune microenvironment in lung adenocarcinoma. *J. Cancer Res. Clin. Oncol.* **148**(3), 565–575. https://doi.org/10.1007/s00432-021-03842- (2022).
34. Poltorak, M., Meinert, I., Stone, J. C., Schraven, B. & Simeoni, L. Sos1 regulates sustained TCR-mediated Erk activation. *Eur. J. Immunol.* **44**(5), 1535–1540. https://doi.org/10.1002/eji.201344046 (2014).
35. Vaquero, J., Lobe, C. & Fouassier, L. Unveiling resistance mechanisms to EGFR inhibitors in cholangiocarcinoma. *Oncotarget* **9**, 37274–37275. https://doi.org/10.18632/oncotarget.26403 (2018).
36. Peraldo-Neia, C. et al. Prognostic and predictive role of EGFR pathway alterations in biliary cancer patients treated with chemotherapy and anti-EGFR. *PLoS One* **13**(1), e0191593. https://doi.org/10.1371/journal.pone.0191593 (2018).
37. Yoon, H., Min, J. K., Lee, J. W., Kim, D. G. & Hong, H. J. Acquisition of chemoresistance in intrahepatic cholangiocarcinoma cells by activation of AKT and extracellular signal-regulated kinase (ERK)1/2. *Biochem. Biophys. Res. Commun.* **405**, 3. https://doi.org/10.1016/j.bbrc.2010.11.130 (2011).
38. De, S., Dermawan, J. K. & Stark, G. R. EGF receptor uses SOS1 to drive constitutive activation of NFκB in cancer cells. *Proc. Natl. Acad. Sci. U S A.* **111**(32), 11721–11726. https://doi.org/10.1073/pnas.1412390111 (2014).
39. Loilome, W. et al. PRKAR1A overexpression is associated with increased ECPKA autoantibody in liver fluke-associated cholangiocarcinoma: application for assessment of the risk group. *Tumour Biol.* **33**(6), 2289–2298. https://doi.org/10.1007/s13277-012-0491-3 (2012).
40. Zheng, Y. et al. Specific genomic alterations and prognostic analysis of perihilar cholangiocarcinoma and distal cholangiocarcinoma. *J. Gastrointest. Oncol.* **12**(6), 2631–2642. https://doi.org/10.21037/jgo-21-776 (2021).
41. Ma, D., Lian, F. & Wang, X. PLCG2 promotes hepatocyte proliferation in vitro via NF-κB and ERK pathway by targeting bcl2, Myc and ccnd1. *Artif. Cells Nanomed. Biotechnol.* **47**, 1:3786–3792. https://doi.org/10.1080/21691401.2019.1669616 (2019).
42. Alvaro, D. et al. Estrogens and insulin-like growth factor 1 modulate neoplastic cell growth in human cholangiocarcinoma. *Am. J. Pathol.* **169**(3), 877–888. https://doi.org/10.2353/ajpath.2006.050464 (2006).
43. Vaquero, J. et al. The IGF2/IR/IGF1R pathway in tumor cells and myofibroblasts mediates resistance to EGFR Inhibition in cholangiocarcinoma. *Clin. Cancer Res.* **24**(17), 4282–4296. https://doi.org/10.1158/1078-0432.CCR-17-3725 (2018).
44. Matallanas, D. et al. Raf family kinases: old dogs have learned new tricks. *Genes Cancer* **2**(3), 232–260. https://doi.org/10.1177/1947601911407323 (2011).

45. West, N. R., Owens, B. M. J. & Hegazy, A. N. The oncostatin M-stromal cell axis in health and disease. *Scand. J. Immunol.* **88**(3), e12694. https://doi.org/10.1111/sji.12694 (2018).
46. Dai, J. et al. SPOP regulates the expression profiles and alternative splicing events in human hepatocytes. *Open. Life Sci.* **18**(1), 20220755. https://doi.org/10.1515/biol-2022-0755 (2023).
47. Ali, A., Nimisha, Sharma, A. K., Mishra, P. K. & Saluja, S. S. Clinical significance of SPOP and APC gene alterations in colorectal cancer in Indian population. *Mol. Genet. Genomics* **298**(5), 1087–1105. https://doi.org/10.1007/s00438-023-02029-x (2023).
48. Xu, J. et al. Properties and clinical relevance of speckle-type POZ protein in human colorectal cancer. *J. Gastrointest. Surg.* **19**, 1484–1496. https://doi.org/10.1007/s11605-015-2767-6 (2015).
49. Zhao, W., Zhou, J., Deng, Z., Gao, Y. & Cheng, Y. SPOP promotes tumor progression via activation of beta-catenin/TCF4 complex in clear cell renal cell carcinoma. *Int. J. Oncol.* **49**, 1001–1008. https://doi.org/10.3892/ijo.2016.3609 (2016).
50. Wan, D. et al. PRKAR2A-derived circular RNAs promote the malignant transformation of colitis and distinguish patients with colitis-associated colorectal cancer. *Clin. Transl Med.* **12** (2), e683. https://doi.org/10.1002/ctm2.683 (2022).
51. Duan, T., Zhou, D., Yao, Y. & Shao, X. The association of aberrant expression of FGF1 and mTOR-S6K1 in colorectal Cancer. *Front. Oncol.* **11**, 706838. https://doi.org/10.3389/fonc.2021.706838 (2021). Erratum in: Front Oncol. 2021;11:792453.
52. Mehta, A. K., Gracias, D. T. & Croft, M. TNF activity and T cells. *Cytokine* **101**, 14–18. https://doi.org/10.1016/j.cyto.2016.08.003 (2018).
53. Uramoto, H., Akyürek, L. M. & Hanagiri, T. A positive relationship between filamin and VEGF in patients with lung cancer. *Anticancer Res.* **30**, 10:3939–3944 (2010).
54. Huang, Y. et al. High expression of ITGA3 promotes proliferation and cell cycle progression and indicates poor prognosis in intrahepatic cholangiocarcinoma. *Biomed. Res. Int.* **2018**, 2352139. https://doi.org/10.1155/2018/2352139 (2018).
55. Ning, P. et al. PLAU plays a functional role in driving lung squamous cell carcinoma metastasis. *Genes Dis.* **11**(2), 554–557. https://doi.org/10.1016/j.gendis.2023.04.010 (2023).
56. Wen, S. C. et al. ets-2 regulates cdc2 kinase activity in mammalian cells: coordinated expression of cdc2 and Cyclin A. *Exp. Cell. Res.* **217**(1), 8–14. https://doi.org/10.1006/excr.1995.1057 (1995).
57. Zabuawala, T. et al. An ets2-driven transcriptional program in tumor-associated macrophages promotes tumor metastasis. *Cancer Res.* **70**(4), 1323–1333. https://doi.org/10.1158/0008-5472.CAN-09-1474 (2010).
58. Szymczyk, J. et al. FGF1 protects FGFR1-overexpressing cancer cells against drugs targeting tubulin polymerization by activating AKT via two independent mechanisms. *Front. Oncol.* **12**, 1011762. https://doi.org/10.3389/fonc.2022.1011762 (2022).
59. Hong, J. et al. Expression of variant isoforms of the tyrosine kinase SYK determines the prognosis of hepatocellular carcinoma. *Cancer Res.* **74**, 6:1845–1856. https://doi.org/10.1158/0008-5472.CAN-13-2104 (2014).
60. Oba, M. et al. CCR7 mediates cell invasion and migration in extrahepatic cholangiocarcinoma by inducing epithelial-mesenchymal transition. *Cancers (Basel)* **15**, 61878. https://doi.org/10.3390/cancers15061878 (2023).
61. Roy, S., Glaser, S. & Chakraborty, S. Inflammation and progression of cholangiocarcinoma: role of angiogenic and lymphangiogenic mechanisms. *Front. Med. (Lausanne)* **6**, 293. https://doi.org/10.3389/fmed.2019.00293
62. Taniai, M. et al. Mcl-1 mediates tumor necrosis factor-related apoptosis-inducing ligand resistance in human cholangiocarcinoma cells. *Cancer Res.* **64**, 10 (2004).
63. Ma, B. et al. Distinct clinical and prognostic implication of IDH1/2 mutation and other most frequent mutations in large duct and small duct subtypes of intrahepatic cholangiocarcinoma. *BMC Cancer* **20**(1), 318. https://doi.org/10.1186/s12885-020-06804-6 (2020).
64. Mehta, A. K., Gracias, D. T. & Croft, M. TNF activity and T cells. *Cytokine* **101**, 14–18. https://doi.org/10.1016/j.cyto.2016.08.003 (2018).
65. Ran., G. H. et al. Natural killer cell homing and trafficking in tissues and tumors: From biology to application. *Signal. Transduct. Target. Ther.* **7**(1), 205. https://doi.org/10.1038/s41392-022-01058-z (2022).
66. Wang, J., Jiang, Y. H., Yang, P. Y., Liu, F. & Increased Collagen Type, V. α2 (COL5A2) in colorectal Cancer is associated with poor prognosis and tumor progression. *Onco Targets Ther.* **14**, 2991–3002. https://doi.org/10.2147/OTT.S288422 (2021).
67. Liu, Q. et al. Oncostatin M expression and TP53 mutation status regulate tumor-infiltration of immune cells and survival outcomes in cholangiocarcinoma. *Aging (Albany NY)* **12**(21), 21518–21543. https://doi.org/10.18632/aging.103936 (2020).
68. Chen, W. et al. Unraveling the heterogeneity of cholangiocarcinoma and identifying biomarkers and therapeutic strategies with single-cell sequencing technology. *Biomed. Pharmacother.* **162**, 114697. https://doi.org/10.1016/j.biopha.2023.114697 (2023).
69. Lin, P. et al. Survival analysis of genome-wide profiles coupled with connectivity map database mining to identify potential therapeutic targets for cholangiocarcinoma. *Oncol. Rep.* **40**(6), 3189–3198. https://doi.org/10.3892/or.2018.6710 (2018).
70. Abell, K. & Watson, C. J. The Jak/Stat pathway: A novel way to regulate PI3K activity. *Cell. Cycle* **4**, 897–900. https://doi.org/10.4161/cc.4.7.1837 (2005).
71. Tang, S. et al. Association analyses of the JAK/STAT signaling pathway with the progression and prognosis of colon cancer. *Oncol. Lett.* **17**(1), 159–164. https://doi.org/10.3892/ol.2018.9569 (2019).
72. Chen, B. et al. JAK1 as a prognostic marker and its correlation with immune infiltrates in breast cancer. *Aging (Albany NY).* **11**(23), 11124–11135. https://doi.org/10.18632/aging.102514 (2019).
73. Pei, Y., Cui, X. & Wang, Y. Regulation of IL-10 expression and function by JAK-STAT in CD8 + T cells. *Int. Immunopharmacol.* **128**, 111563. https://doi.org/10.1016/j.intimp.2024.111563 (2024).
74. Shen, K. et al. The expression landscape of JAK1 and its potential as a biomarker for prognosis and immune infiltrates in NSCLC. *BMC Bioinform.* **22**, 1471. https://doi.org/10.1186/s12859-021-04379-y (2021).
75. Suksawat, M. et al. Upregulation of endothelial nitric oxide synthase (eNOS) and its upstream regulators in *Opisthorchis viverrini* associated cholangiocarcinoma and its clinical significance. *Parasitol. Int.* **66**, 4:486–493. https://doi.org/10.1016/j.parint.2016.04.008 (2017).
76. Alwithenani, A. I. & Althubiti, M. A. Systematic analysis of spleen tyrosine kinase expression and its clinical outcomes in various cancers. *Saudi J. Med. Med. Sci.* **8**(2), 95–104. https://doi.org/10.4103/sjmms.sjmms_300_19 (2020).
77. Guittard, G. et al. Absence of both Sos-1 and Sos-2 in peripheral CD4(+) T cells leads to PI3K pathway activation and defects in migration. *Eur. J. Immunol.* **45**, 8. https://doi.org/10.1002/eji.201445226 (2015).
78. Alem, D. et al. Translational relevance of SOS1 targeting for KRAS-mutant colorectal cancer. *Mol. Carcinog.* **62**(7), 1025–1037. https://doi.org/10.1002/mc.23543 (2023).
79. Li, Y., Yin, Y., He, Y., He, K. & Li, J. SOS1 regulates HCC cell epithelial-mesenchymal transition via the PI3K/AKT/mTOR pathway. *Biochem. Biophys. Res. Commun.* **637**, 161–169. https://doi.org/10.1016/j.bbrc.2022.11.015 (2022).
80. Li, Q. et al. High integrin A3 expression is associated with poor prognosis in patients with non-small cell lung cancer. *Transl Lung Cancer Res.* **9**(4), 1361–1378. https://doi.org/10.21037/tlcr-19-633 (2020).
81. Wu, A. et al. Integrated analysis of prognostic and immune associated integrin family in ovarian cancer. *Front. Genet.* **11**, 705. https://doi.org/10.3389/fgene.2020.00705 (2020).
82. Zheng, Q., Zhang, B., Li, C. & Zhang, X. Overcome drug resistance in cholangiocarcinoma: New insight into mechanisms and refining the preclinical experiment models. *Front. Oncol.* **12**, 850732. https://doi.org/10.3389/fonc.2022.850732 (2022).
83. Sridharan, V. et al. FGFR mRNA expression in cholangiocarcinoma and its correlation with FGFR2 fusion status and immune signatures. *Clin. Cancer Res.* **28**(24), 5431–5439. https://doi.org/10.1158/1078-0432.CCR-22-1244 (2022).
84. Krook, M. A. et al. Efficacy of FGFR inhibitors and combination therapies for acquired resistance in FGFR2-fusion cholangiocarcinoma. *Mol. Cancer Ther.* **19**(3), 847–857. https://doi.org/10.1158/1535-7163.MCT-19-0631 (2020).

85. Zamai, L. et al. Natural killer (NK) cell-mediated cytotoxicity: differential use of TRAIL and fas ligand by immature and mature primary human NK cells. *J. Exp. Med.* **188**(12), 2375–2380. https://doi.org/10.1084/jem.188.12.2375 (1998).
86. Matsuzawa, A. et al. ROS-dependent activation of the TRAF6-ASK1-p38 pathway is selectively required for TLR4-mediated innate immunity. *Nat. Immunol.* **6**(6), 587–592. https://doi.org/10.1038/ni1200 (2005).
87. Ghafouri-Fard, S. et al. 5-Fluorouracil: A narrative review on the role of regulatory mechanisms in driving resistance to this chemotherapeutic agent. *Front. Oncol.* **11**, 658636 (2021).
88. Taïeb, J. et al. Optimization of 5-fluorouracil (5-FU)/cisplatin combination chemotherapy with a new schedule of leucovorin, 5-FU and cisplatin (LV5FU2-P regimen) in patients with biliary tract carcinoma. *Ann. Oncol.* **13**(8), 1192–1196 (2002).
89. Siebenhüner, A. R. et al. Adjuvant treatment of resectable biliary tract cancer with cisplatin plus gemcitabine: A prospective single center phase II study. *BMC Cancer***18**(1), 72 (2018).
90. Kotawong, K., Chajaroenkul, W., Roytrakul, S., Phaonakrop, N. & Na-Bangchang, K. The proteomics and metabolomics analysis for screening the molecular targets of action of beta-eudesmol in cholangiocarcinoma. *Asian Pac. J. Cancer Prev.* **22**, 3:909–918. https://doi.org/10.31557/APJCP.2021.22.3.909 (2021).
91. Mathema, V. B., Chaijaroenkul, W., Karbwang, J. & Na-Bangchang, K. Growth inhibitory effect of β-eudesmol on cholangiocarcinoma cells and its potential suppressive effect on heme oxygenase-1 production, STAT1/3 activation, and NF-κB downregulation. *Clin. Exp. Pharmacol. Physiol.* **44**(11), 1145–1154. https://doi.org/10.1111/1440-1681.12818 (2017).

Author contributions

T.S.: Conceptualization, data curation, validation, formal analysis, methodology, writing-original draft, interpretation. E.V.: Experimental study, W.C.: Experimental study. N.T.: Experimental study. K.N.: Conceptualization, data curation, funding acquisition, supervision, project administration, writing—review, and editing. All authors reviewed the manuscript.

Funding

This research project was supported by the Thailand Science Research and Innovation Fundamental Fund Fiscal Year 2023 and Thammasat University (Chulabhorn International College of Medicine, Center of Excellence in Pharmacology and Molecular Biology of Malaria and Cholangiocarcinoma). Kesara Na-Bangchang is funded by the National Research Council of Thailand (NRCT): Contract number N42A671041. All funders have no roles for publication.

Declarations

Competing interests

The authors declare no competing interests.

Ethical approval and consent to participate

This project has approval from the Human Research Ethics Committee of Sakol Nakorn hospital (No. 049/2563). All participants signed written informed consent forms prior to enrollment.

Additional information

Supplementary Information The online version contains supplementary material available at https://doi.org/10.1038/s41598-025-91968-z.

Correspondence and requests for materials should be addressed to K.N.-B.